HOLLOW-CYLINDER WAVEGUIDE ISOLATORS FOR USE AT MILLIMETER WAVELENGTHS*

M. Kanda** and W. C. May
University of Colorado
Department of Electrical Engineering
Boulder, Colorado 80302

Abstract

The device considered in this study is a semiconductor waveguide isolator consisting of a hollow column of a semiconductor mounted coaxially in a circular waveguide in a longitudinal dc magnetic field. An elementary and physical analysis based on the excitation of plane waves in the guide and a more rigorous mode matching analysis are presented. These theoretical predictions are compared with experimental results for an InSb isolator at 94GHz and 75°K.

* This work was supported in part by NASA under Grant NGR 06-003-088.

** M. Kanda is now with the National Bureau of Standards, Noise and Interference Section, Electromagnetics Division, Boulder, Colorado 80302.

HOLLOW-CYLINDER WAVEGUIDE ISOLATORS FOR USE AT MILLIMETER WAVELENGTHS*

M. Kanda** and W. G. May
University of Colorado
Department of Electrical Engineering
Boulder, Colorado 80302

I. INTRODUCTION

The purpose of this paper is to present a theoretical study of a semiconductor waveguide isolator of new geometry and the experimental results for an InSb isolator at 94 GHz and 75°K.

The propagation characteristics of em waves in a circular waveguide partially filled with a plasma have been investigated extensively examining the effect of a plasma upon waveguide modes. For example, R. N. Carlile[1] measured the propagation constants of the TE_{11} modes in a cylindrical waveguide partially filled with a gaseous plasma in a longitudinal dc magnetic field and observed that right and left circularly polarized (cp) waves travel with different propagation constants. The theoretical and experimental study of a circular 35 GHz waveguide containing a coaxial InSb rod was done extensively by B. R. McLeod and W. G. May[2,3,4].

The configuration to be studied here, shown in Fig. 1, has a hollow plasma column in a circular waveguide. This geometry is more practical to construct than the rod configuration for millimeter waveguides. The theoretical analysis will be in two parts: First, a heuristic argument based on the excitation of plane waves in the guide is presented. Second,

---

* This work was supported in part by NASA under Grant NGR 06-003-088.

** M. Kanda is now with the National Bureau of Standards, Noise and Interference Section, Electromagnetics Division, Boulder, Colorado 80302.

a more rigorous mode matching analysis (henceforth abbreviated MMA) is given.

II. FORMULATION OF THE PROBLEM

With a longitudinal dc magnetic field on the plasma column, the total dielectric constant of the material seen by the em waves is due to both lattice and free carriers and depends on the direction of the circular polarization (cp) with respect to the longitudinal magnetic field. The total relative dielectric constant has the form[5]:

$$K_{\pm} = K_{\perp} \pm jK_{\times} = K'_{\pm} + jk''_{\pm} \quad , \qquad (1)$$

where

$$K'_{\pm} = K_L - \frac{\omega_p^2 \tau^2 (\omega \pm \omega_c)}{\omega[1+\tau^2(\omega\pm\omega_c)^2]} \quad , \qquad (2)$$

$$K''_{\pm} = - \frac{\omega_p^2 \tau}{\omega[1+\tau^2(\omega\pm\omega_c)^2]} \quad , \qquad (3)$$

and

$$\omega_p^2 = \frac{ne^2}{m^*\varepsilon_o} \quad , \qquad (4)$$

$$\omega_c = \frac{eB_o}{m^*} \quad . \qquad (5)$$

Here K_L is the relative static lattice dielectric constant of the magneto-plasma, and τ is the carrier relaxation time. The subscript $\pm$ refers to the left and right cp components in the direction of the dc magnetic field. For suitable choice of parameters, K'_- could be relatively large and K'_+ very low or even negative, and $K''_{\pm}$ small. This possibility is put to use in an isolator as described below by exciting a right or left cp wave in the circular waveguide containing an annular plasma column in a longitudinal magnetic field, as shown in Fig. 1.

II-1. APPROXIMATE THEORY FOR ATTENUATION COEFFICIENT

In this section we develop a simple physical picture from which the performance of the structure of Fig. 1 can be estimated. Using a heuristic argument, we will find the ratio of the electric field strength in the annular plasma column to the field in the center section of air-filled region. It is assumed that the fields both in the center section of the air-filled region and in the annular plasma column are plane waves of approximately the TE_{11} mode pattern. The amplitudes of fields in the two regions can be, however, drastically different and depend on the dielectric constant of each region. We further assume that a simple static analysis will suffice to determine these relative amplitudes. Of course, the above assumptions are not truly valid and will not be used in the more rigorous MMA in the next section.

The simple static analysis gives for the ratio of the field concentrations:

$$\frac{E_i}{E_o} = \frac{2}{1 + \frac{1}{K}} \quad , \qquad (6)$$

where K is the ratio of the relative dielectric constants of the outer and inner media, and E_i and E_o are the "uniform" fields in the inner and outer regions. Since the inner region is empty, K will be interpreted as K_+, Eq. 1, for cp waves.

If the material parameters and magnetic field are such that $\omega_c >> \omega$, $1/\tau$ and if the dc magnetic field is adjusted so that K_+' as in (1) is close to zero (at least $K_+' << K_L$), it appears reasonable from (6) that the left cp waves are strongly excited in the outer region, the annular plasma column. Thus, the wave propagates almost exclusively through the plasma, and because of the lossy part of the dielectric constant of the plasma, much of

the left cp wave will be absorbed by the plasma and dissipated as heat. On the other hand, the same em wave traveling in the opposite direction with respect to the longitudinal dc magnetic field is right cp. It is predicted from (6) that this wave is largely excluded from the annular plasma column because K'_- will be large ($\sim 2K_L$, for InSb, 32), and with $K'_- > K''_-$, the wave will be only slightly absorbed by the plasma.

Let us examine the attenuation coefficient using the approximate model discussed above. Consider an infinitely long annular plasma column placed in a uniform em field with the propagation direction parallel to the axis of the column. Assuming that the transverse fields in the annular plasma column are approximately uniform for both polarizations of the em waves, the power dissipation per unit length in the plasma annulus is

$$P_{diss} = \frac{1}{2}\sigma_\pm |E_o|^2 A_o = \frac{1}{2}\omega\varepsilon_o K''_\pm |E_o|^2 A_o \quad , \tag{7}$$

where E_o is the field inside the annular plasma column, A_o is its cross-sectional area and $\sigma_\pm$ is the effective conductivity of the plasma, $\omega\varepsilon_o K''_\pm$. From the foregoing discussion, the field inside the plasma column is also assumed to be a uniform TE mode, and the power flow through the plasma column, P_o, is then approximately given by

$$P_o = \frac{1}{2}\frac{|E_o|^2}{\eta_o} A_o = \frac{1}{2}\frac{R_e\sqrt{K_\pm}}{Z_o} |E_o|^2 A_o \left[1-\left(\frac{\lambda}{\lambda_c}\right)^2\right]^{\frac{1}{2}} \quad , \tag{8}$$

where η_o is the impedance of the TE mode in the column, $Z_o = 377$ ohms, and λ_c is the guide cutoff wavelength. Similarly the power flow through the center air-filled region, P_i, is given crudely by

$$P_i = \frac{1}{2}\frac{|E_i|^2}{Z_o} A_i \quad , \tag{9}$$

where E_i is the field in this region and A_i is the area of its cross section. The approximate attenuation coefficient, $\alpha_\pm$, due to absorption in the plasma is found by dividing the dissipated power (7) by the total power flow $P_o + P_i$

and is found to be:

$$\alpha_{\pm} = \frac{1}{2} \frac{\omega\varepsilon_o Z_o K_{\pm}'' |1+K_{\pm}|^2 A_o}{R_e\sqrt{K_{\pm}}\,|1+K_{\pm}|^2 [1-(\frac{\lambda}{\lambda_c})^2]\, A_o + 4|K_{\pm}|^2 A_i}^{1/2} \quad . \qquad (10)$$

This expression will be evaluated and compared to the more accurate expression derived from the MMA in the next section.

II-2. MODE MATCHING ANALYSIS FOR THE BOUNDARY VALUE PROBLEM

The general calculations of the reflection and transmission coefficients of a finite-length section of the annular magnetoplasma column as in Fig. 1 consist of the following two steps:

1) Determination of the propagation constants of the gyromagnetic modes in the section of the annular magnetoplasma column, $0 \le z \le \ell$.

2) Use of these propagation constants to match the boundary conditions at the ends of plasma column, $z=0, \ell$.

The radial boundary conditions are that the tangential components of E are zero at r=b and that the tangential components of E and H are continuous at r=a. The characteristic equation turns out to be a 6×6 determinant (see discussion in Appendix A). The problem of matching fields at the ends of the plasma column is quite complicated since a single incident mode can excite a number of gyromagnetic modes in the plasma section and these, in turn, excite a number of TE and TM modes in the empty waveguide, and these higher modes must be included in applying the boundary conditions. Furthermore, the gyromagnetic modes do not form orthogonal sets due to the existence of loss in the plasma [6], and we use the point matching method to compute

approximately the reflection and transmission coefficients at the ends of the plasma column, by matching boundary conditions at only a finite number of points over the cross section. This formulation becomes increasingly exact by increasing the number of modes considered and the number of matching points chosen. The overall attenuation due to the finite section of the annular plasma column is then calculated from the transmission coefficient of the dominant mode at the end of the plasma column.

The details of the calculations are given in Appendix B, and some numberical results will be presented in §IV below.

III. EXPERIMENTAL PROCEDURE

The material chosen for the solid state plasma was n-type InSb. This material had $n = 2.8\times10^{14}/cm^3$ and $\mu = 5.2\times10^5 cm^2/V\text{-sec}$ at the operating temperature (75°K), and we assumed that $K_L = 16.0$ and $m^* = 0.014m_o$.

The isolators tested consisted of two transitions and the test section shown in Fig. 2. The transitions convert the TE_{10} mode propagating in the rectangular waveguide into the cp TE_{11} mode in the circular waveguide. The test section contains the annular column of n-type InSb, which was cut by using an ultra-sonic drill and polished chemically in a bromine and methanol etch. The small opening between the column and the circular waveguide wall was filled with highly conducting silver paint, and styrofoam filled the center section. The devices were placed in a longitudinal dc magnetic field using a 6-inch Varian magnet with a 2-inch gap. A styrofoam Dewar surrounding the semiconductor was filled with the liquid nitrogen which was not allowed to enter the test section. The microwave system was conventional with a precision attenuator. A block diagram of the experimental set-up is shown in Fig. 3.

V. DISCUSSION OF EXPERIMENTAL AND THEORETICAL RESULTS

The experimental and theoretical results of propagation characteristics for a circular waveguide containing an annular InSb column in a longitudinal dc magnetic field are presented in this section. The results calculated from the approximate theory of II-1 and from the MMA of II-2 are given. The validity of the assumptions made and the correlation between the experimental and theoretical results are discussed. Figs. 4 and 5 show the attenuation results for two lengths ℓ of InSb. Only losses within the test section are included.

IV-1. COMPARISON WITH THE APPROXIMATE THEORY

The calculated attenuation curves derived from the approximate theory of II-1 are shown dotted in Fig. 4 and 5. This figure shows that approximate theory gives a qualitative agreement with the corresponding experimental results for a low longitudinal dc magnetic field up to approximately 6 kG indicating the approximate conditions for best isolation. The assumption of a uniform plane wave propagating in the section of the annular InSb column appears to be crudely correct, justifying the physical argument given in §II-1 for the smaller magnetic fields. For the case of higher fields, MMA of the boundary value problem showed that the excitation of higher gyromagnetic modes becomes significant, and a large deviation of the electric field from the TE_{11} mode pattern is expected. Thus there is considerable inaccuracy in the approximate theory. The approximate theory did not account for the transition between the empty waveguide and the guide in which the annular InSb column was mounted, nor did it account for any reflections, and thus only qualitative agreement between theoretical and experimental results could be expected.

IV-2. COMPARISON WITH MODE MATCHING ANALYSIS

The first step of MMA was to determine the propagation constants of the gyromagnetic modes. Since the characteristic equation is quite complicated, an iterative root-finding technique was employed to find the propagation constants. The real and imaginary parts of the propagation constants for both right and left polarizations were obtained by computer to three place accuracy.

The resulting propagation constants were utilized to match the boundary conditions at the ends of the plasma column. This second step determines the amplitudes of the reflection and transmission coefficients of the gyromagnetic modes and of the empty waveguide modes. In the present case, four gyromagnetic modes in the section of the InSb column and two TE and two TM modes in the empty waveguide were taken into account. Point matching was employed at r=0.3 and 0.7mm to solve the inhomogeneous linear equations of order 16. The overall attenuation due to the various lengths of the InSb columns was evaluated from the transmission coefficients of TE_{11} circular mode at the ends of the column and is shown in Figs. 4 and 5 by the solid lines. The general agreement between the experimental and the theoretical results is quite good. The boundary conditions are imposed at only four points at the ends of the plasma column by taking into account only four gyromagnetic modes in the magnetoplasma section and four higher excited modes in the empty waveguide section. It is, however, expected that, although the inclusion of higher excited modes as well as the dominant modes is essential in a rigorous treatment of the boundary conditions at the ends of the plasma column, the convergence is fairly rapid [7]. Thus small discrepancy between theoretical and experimental results appear to be mainly due to lack of perfect cylindrical symmetry in the experimental setup.

The calculated reflection coefficients of the incident TE_{11} mode at the ends of the plasma column show that the devices are absorbing rather than reflecting the microwave power to achieve the attenuation obtained experimentally. A small amount of the reflected wave is linearly polarized in a horizontal plane, and thus is absorbed by the resistance card placed behind the polarizer. Of course, it could be possible to prevent this reflection by careful design of a matching section such as a conical taper or an end cap of dielectric material whose dielectric constant is chosen so as to provide an impedance match at the ends of plasma column.

V. CONCLUSIONS

Theoretical and experimental investigations were performed for the purpose of the utilization of nonreciprocal behavior in the solid state magnetoplasma for the development of millimeter waveguide isolators. The present work demonstrated the feasibility of making an isolator using a coaxial annular column of n-type InSb in a circular waveguide cooled to 75°K. The plasma column isolator is relatively easy to construct in small circular waveguide with the power absorbing medium easily heat sunk. No attempt was made to optimize the front-to-back attenuation ratio, and the efficiency of the device should be readily improved.

APPENDIX A

CHARACTERISTIC EQUATION FOR CIRCULAR WAVEGUIDE CONTAINING ANNULAR PLASMA COLUMN

This appendix outlines the boundary value problem that results from the configuration shown in Fig. 1.

The appropriate solutions of the wave equations for the longitudinal field components for r<a are

$$E_z^o = UJ_m(qr)e^{jm\phi-\Gamma z} \quad , \tag{11}$$

and

$$H_z^o = VJ_m(qr)e^{jm\phi-\Gamma z} \quad , \tag{12}$$

where U and V are arbitrary, complex constants and Γ the complex propagation constant. Corresponding transverse E field components for r<a are

$$E_r^o = \left[-U\frac{\Gamma}{q}J_m'(qr) - V\frac{\omega\mu_o m}{q^2 r}J_m(qr)\right] e^{jm\phi-\Gamma z} \quad , \tag{13}$$

$$E_\phi^o = \left[-U\frac{jm}{q^2 r}J_m(qr) + Vj\frac{\omega\mu_o}{q}J_m'(qr)\right] e^{jm\phi-\Gamma z} \quad , \tag{14}$$

with similar expressions for H.

In the region of the annular plasma column a<r<b, Maxwell's equations yield the coupled wave equations:

$$\nabla_T^2 E_z + aE_z = bHz \quad , \tag{15}$$

$$\nabla_T^2 H_z + cH_z = dE_z \quad , \tag{16}$$

where a, b, c, d can be defined in terms of Γ and the plasma dielectric tensor components. Assuming solutions of the form $\exp(-jp\cdot r_T)$, these can be solved giving the dispersion equation:

$$p^4 - (a+c)p^2 + (ac-bd) = 0 \quad , \tag{17}$$

The longitudinal E field inside the annular plasma (a<r<b) is

$$E_z = [AJ_m(p_1 r) + BN_m(p_1 r) + CJ_m(p_2 r) + DN_m(p_2 r)]e^{jm\phi - \Gamma z} \quad , \tag{18}$$

with a similar expression for H_z, and A, B, C and D are arbitrary, complex constants with similar but more complicated expressions for the other components of E and H.

Now the boundary conditions at the plasma surface (r=a) shall be taken as the continuity of the tangential E and H fields; (4 equations). Also at the boundary of the perfect conductor waveguide wall (r=b), tangential E and H fields are zero; (2 more equations). In order to have non-trivial solutions of A, B, C, D, U and V, the 6×6 determinant of these coefficients for the 6 equations must be zero. The details will not be published here due to space limitations but will be supplied upon request to the authors [8].

APPENDIX B

MATCHING FIELDS AT THE ENDS OF THE MAGNETOPLASMA COLUMN

For a plasma section of finite length, one is confronted with the problem of matching fields at the ends of the plasma column. Let us consider the configuration shown in Fig. 1 when the incident wave is TE_{11}.

One component of the H field in region 1 is

$$H_z = J_m(q_1^E r)e^{jm\phi-\Gamma_1^E z} + \sum_n -R_{n1}^E J_m(q_n^E r)e^{jm\phi+\Gamma_n^E z} \quad , \tag{19}$$

where R_{n1}^E is a reflection coefficient, with similar expressions for the other components of H and for E. The mode propagation constant, Γ_n^E, is determined from the characteristic equation of the TE wave, i.e.,

$$J_m'(q_n^E b) = 0 \quad , \tag{20}$$

where

$$q_n^{E^2} = \Gamma_n^{E^2} + k_o^2 \quad . \tag{21}$$

In the plasma a<r<b, one component of E field is

$$E_z = \sum_n T_{n2}\Big[A_n J_m(p_1 r) + B_n N_m(p_1 r) + C_n J_m(p_2 r) + D_n N_m(p_2 r)\Big] e^{jm\phi-\Gamma_n z} + \sum_n R_{n2}\Big[A_n J_m(p_1 r) + B_n N_m(p_1 r) + C_n J_m(p_2 r) + D_n N_m(p_2 r)\Big] e^{jm\phi+\Gamma_n z} \quad , \tag{22}$$

and for o<r<a

$$E_z = \sum_n T_{n2}\, U_n J_m(q_n r)e^{jm\phi-\Gamma_n z} + \sum_n -R_{n2} V_n J_m(q_n r)e^{jm\phi+\Gamma_n z} \quad , \tag{23}$$

here R_{ni} and T_{ni} are mode reflection and transmission coefficients, with imilar and far more complicated expressions for the other components of E and H.

Similarly, in Region 3

$$H_z = \sum_n T^E_{n3} J_m(q^E_n r) e^{jm\phi - \Gamma^E_n z} , \qquad (24)$$

with corresponding expressions for the other field components of H and E.

The reflection and transmission coefficients for the n^{th} TE (or TM) mode in the i^{th} region, R^E_{ni} and T^E_{ni} (R^M_{ni} and T^M_{ni}) are determined by the point-matching method. The overall attenuation, α, expressed in dB due to the finite section of the annular plasma column is then calculated from the transmission coefficient of the dominant mode at the end of the plasma column:

$$\alpha = -20 \log|T^E_{13}| \qquad (25)$$

REFERENCES

1. Carlile, R.N., "Quasi-TE_{11} Modes in an Anisotropic Plasma Waveguide", IEEE Trans. on Microwave Theory and Techniques, Vol. MTT-14, pp. 350-351 (July, 1966).

2. McLeod, B.R., Quasi-Optical and Waveguide Applications of Indium Antimonide, Ph.D. Thesis, University of Colorado (May 1968).

3. May, W.G. and B.R. McLeod, "A Waveguide Isolator Using InSb", IEEE Trans. on Microwave Theory and Techniques, Vol. MTT-16, pp. 877-878 (Oct. 1968).

4. McLeod, B.R. and W. G. May, "A 35 GHz Isolator Using a Coaxial Solid State Plasma in a Longitudinal Magnetic Field", IEEE Trans. on Microwave Theory and Techniques, Vol. MTT-19, No. 6, pp. 510-516 (June 1971).

5. Allis, W.P., S. J. Buchshaum and A. Bers, Waves in Anisotropic Plasmas, The M.I.T. Press, Cambridge, Mass. (1963).

6. Clarricoats, P.J.B., Private Communication (1970).

7. Champlin, K.S., G.H. Glover and J.W. Holm-Kennedy, "Plasma-Filled Waveguide with Axial Magnetization. II. Scattering by a Section of Finite Length", J. Appl. Phys., Vol. 40, No. 9, pp. 3538-3544 (Aug. 1969).

8. Kanda, M., Study and Applications of Non-Reciprocal Behavior in Solid State Magnetoplasmas at Millimeter and Submillimeter Wavelengths, Ph.D. Thesis, University of Colorado (July 1971).

FIGURE CAPTIONS

Figure 1. Circular Waveguide Containing an Annular InSb Column

Figure 2. Waveguide Isolator Containing Annular Plasma Column

Figure 3. Block Diagram of Experiment Set-up

Figure 4. Theoretical and Experimental Results for Hollow InSb Waveguide Isolator
[Geometry of 94 GHz InSb Waveguide Isolator is shown in Fig. 2 with ℓ=0.762mm.]

Figure 5. Theoretical and Experimental Results for Hollow InSb Waveguide Isolator
[Geometry of 94 GHz InSb Waveguide Isolator is shown in Fig. 2 with ℓ=1.524mm.]

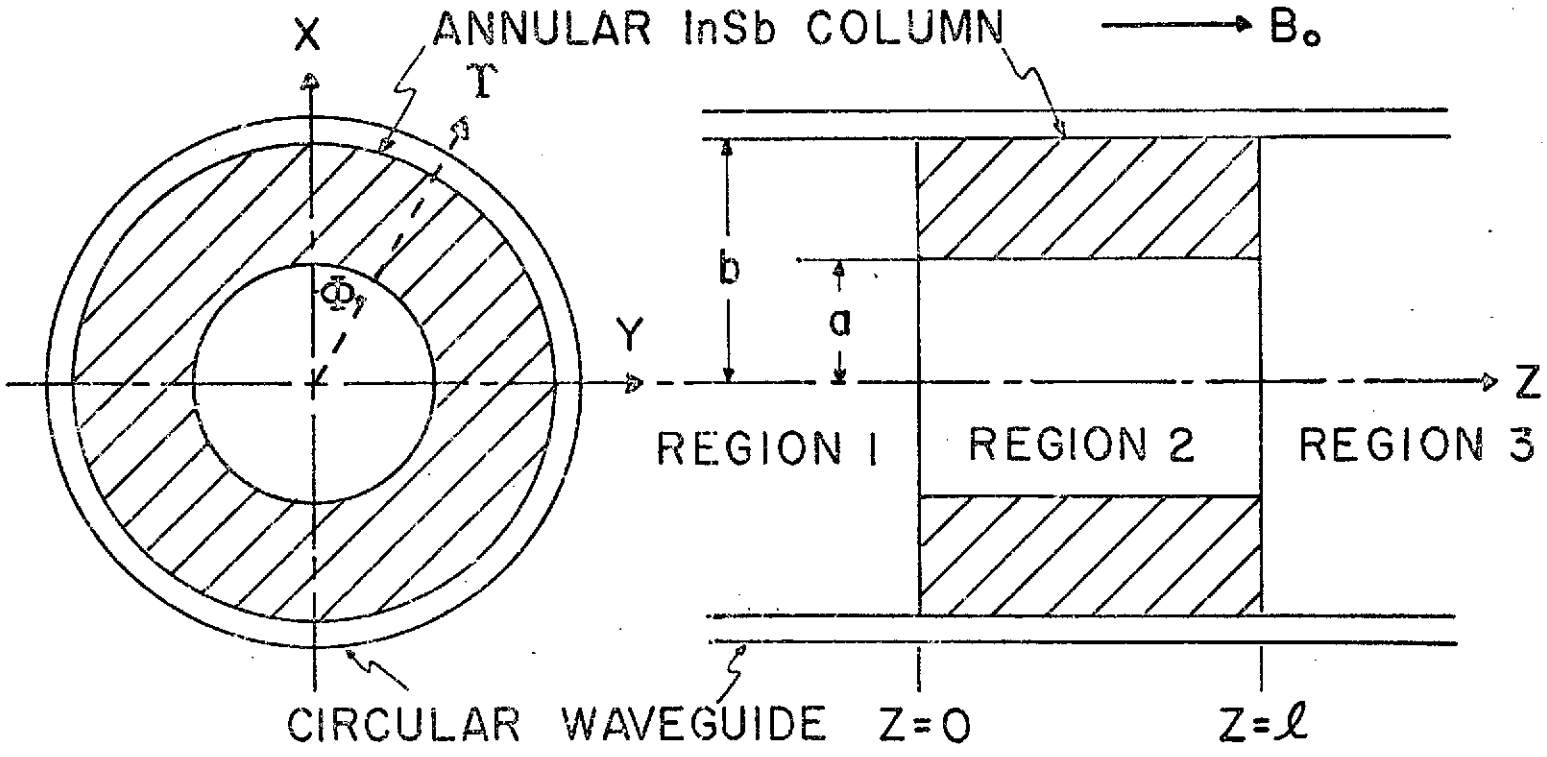
X
ANNULAR InSb COLUMN
B₀
r
Φ₁
Y
b
a
Z
REGION 1
REGION 2
REGION 3
CIRCULAR WAVEGUIDE
Z=0
Z=ℓ

FIGURE 1

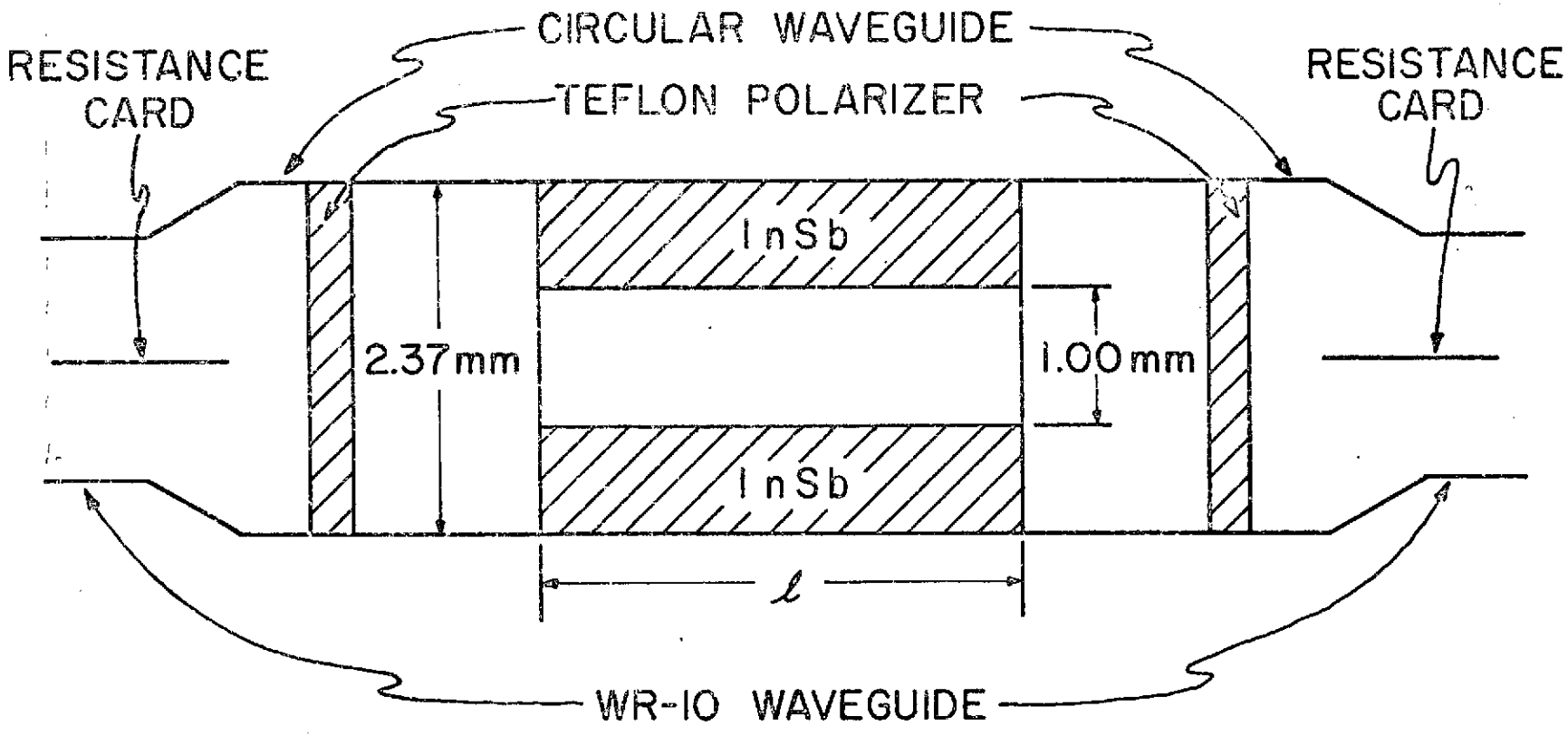
CIRCULAR WAVEGUIDE
RESISTANCE CARD
TEFLON POLARIZER
RESISTANCE CARD
InSb
2.37mm
1.00mm
InSb
ℓ
WR-10 WAVEGUIDE

FIGURE 2

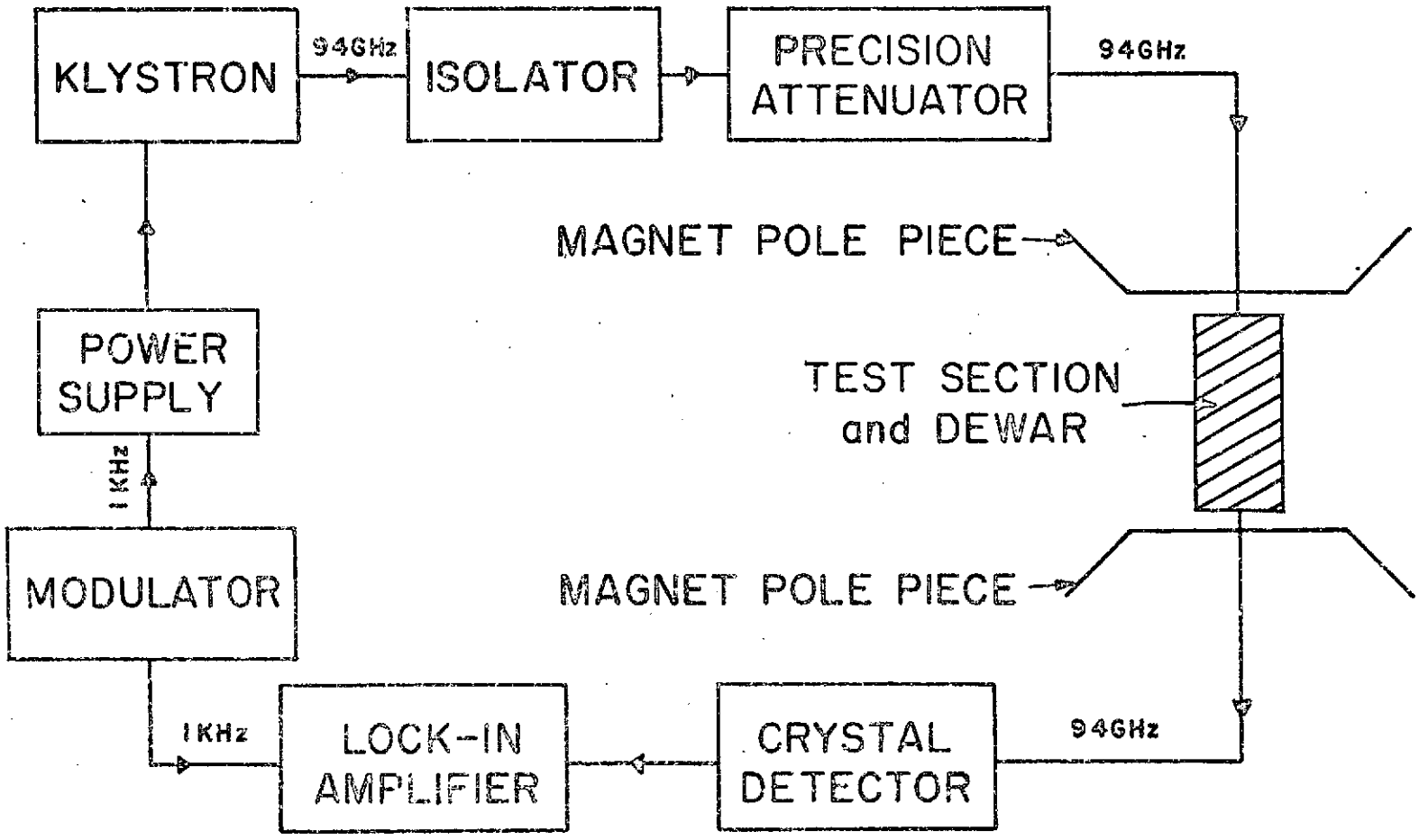
KLYSTRON
94GHz
ISOLATOR
PRECISION ATTENUATOR
94GHz
MAGNET POLE PIECE
POWER SUPPLY
TEST SECTION and DEWAR
1 KHz
MODULATOR
MAGNET POLE PIECE
1 KHz
LOCK-IN AMPLIFIER
CRYSTAL DETECTOR
94GHz

FIGURE 3

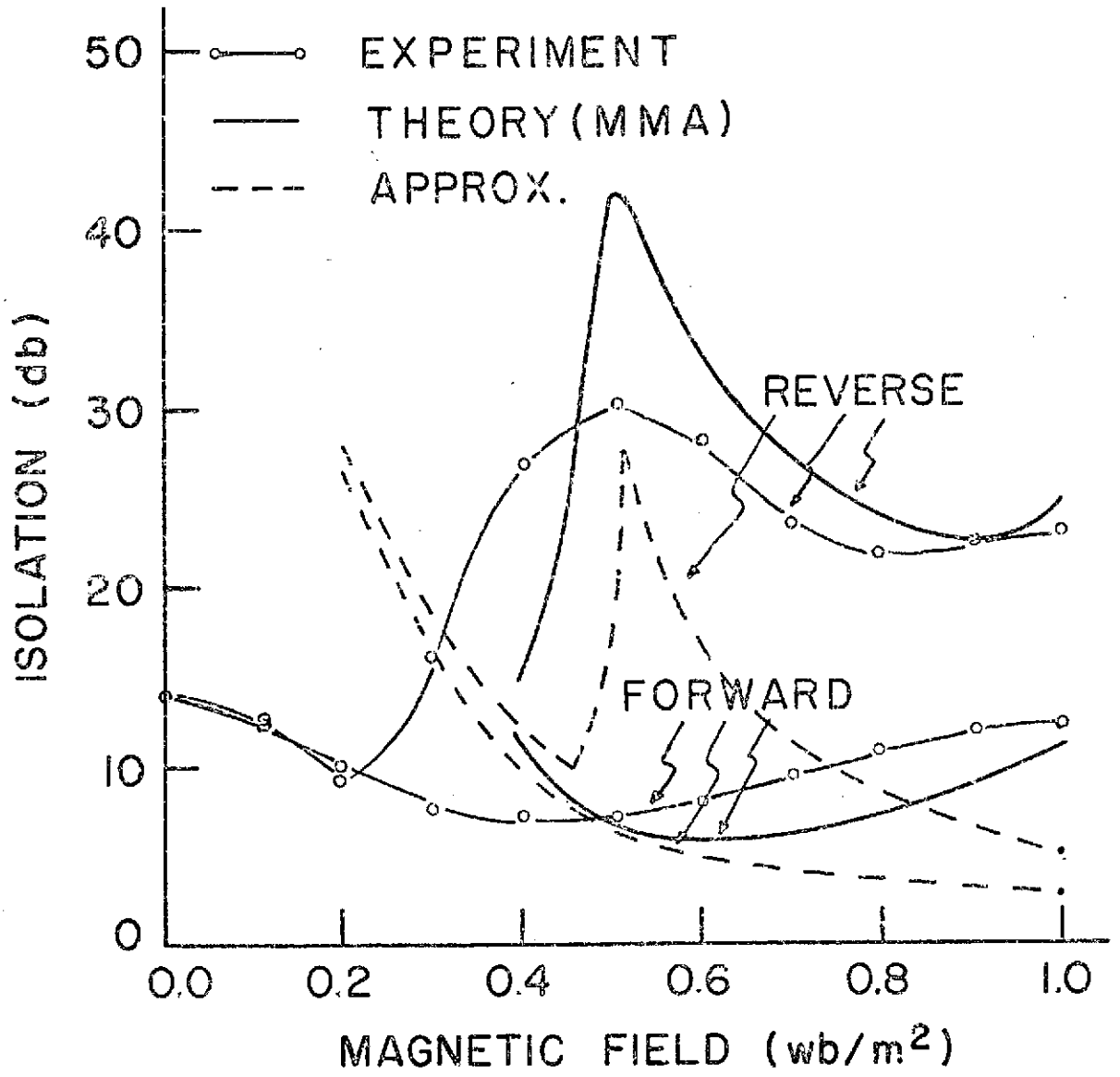
EXPERIMENT
THEORY (MMA)
APPROX.
REVERSE
FORWARD
ISOLATION (db)
50
40
30
20
10
0
0.0
0.2
0.4
0.6
0.8
1.0
MAGNETIC FIELD (wb/m²)

FIGURE 4

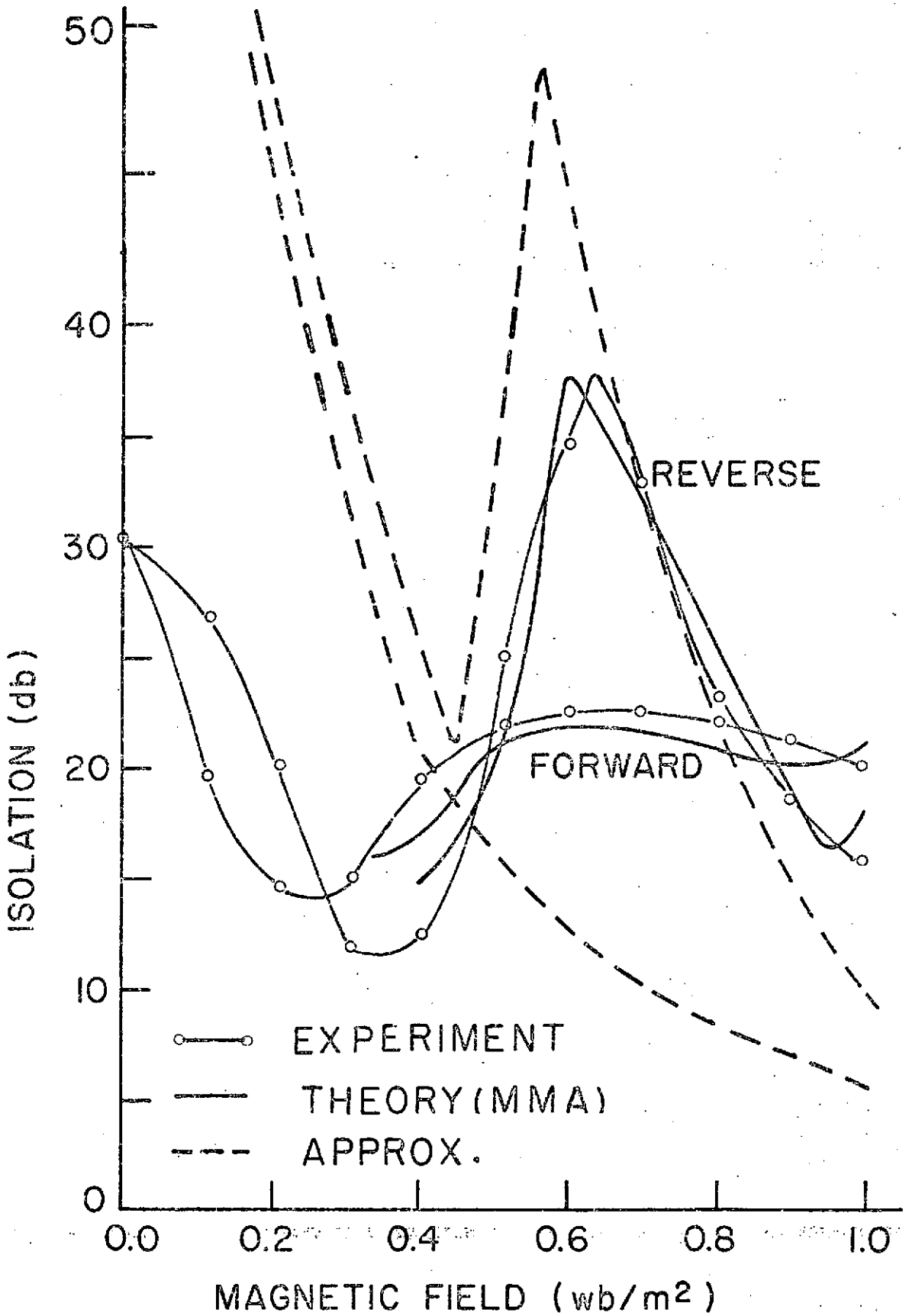
50
40
30
20
10
0
ISOLATION (db)
REVERSE
FORWARD
EXPERIMENT
THEORY (MMA)
APPROX.
0.0
0.2
0.4
0.6
0.8
1.0
MAGNETIC FIELD (wb/m²)

FIGURE 5